JOURNAL OF GEOPHYSICAL RESEARCH, VOL. 112, D04306, doi:10.1029/2006JD007369, 2007

Methane carbon isotope effects caused by atomic chlorine in the marine boundary layer: Global model results compared with Southern Hemisphere measurements

W. Allan,[1] H. Struthers,[2] and D. C. Lowe[1]

Received 4 April 2006; revised 24 August 2006; accepted 5 October 2006; published 22 February 2007.

[1] Recent measurements of the apparent kinetic isotope effect (KIE) of the methane (CH_4) atmospheric sink in the extratropical Southern Hemisphere (ETSH) have shown the apparent KIE to be larger in magnitude than expected if the sink were the hydroxyl radical ($OH^\bullet$) alone. We present results from simulations using the U.K. Met Office's Unified Model (UM) to evaluate whether atomic chlorine ($Cl^\bullet$) in the marine boundary layer (MBL) could give this effect. We modify the UM to include sources of $^{12}CH_4$ and $^{13}CH_4$, soil and stratospheric sinks, and a tropospheric $OH^\bullet$ sink. Also included is a $Cl^\bullet$ sink in the MBL with a large seasonal cycle and a constant mean value ($Cl^\bullet_{mean}$) in latitude. We show that analysis of the simulated seasonal cycles in CH_4 mixing ratio and $\delta^{13}C$ give an accurate estimate of the $OH^\bullet$ KIE at ETSH midlatitudes. The apparent KIE of the combined $OH^\bullet$ and $Cl^\bullet$ sink increases in magnitude as $Cl^\bullet_{mean}$ increases. The experimentally measured values of apparent KIE in the ETSH midlatitudes of −15‰ in 1994–1996 and −7‰ in 1998–2000 are attained with MBL $Cl^\bullet_{mean}$ values of 28×10^3 atoms cm^{-3} and 9×10^3 atoms cm^{-3}, respectively (although we consider the latter to be a lower bound). We suggest that 18×10^3 atoms cm^{-3} is a reasonable midrange estimate of $Cl^\bullet_{mean}$ in the MBL. This value results in a $Cl^\bullet$ sink strength of 25 Tg y^{-1} (range 13–37 Tg y^{-1}) and an enrichment in $\delta^{13}C$ of atmospheric CH_4 by 2.6‰ (range 1.4–3.8‰). This sink strength is significant but has not yet been included in global CH_4 budgets.

Citation: Allan, W., H. Struthers, and D. C. Lowe (2007), Methane carbon isotope effects caused by atomic chlorine in the marine boundary layer: Global model results compared with Southern Hemisphere measurements, *J. Geophys. Res.*, *112*, D04306, doi:10.1029/2006JD007369.

1. Introduction

[2] The mean mixing ratio of methane (CH_4) in the atmosphere has more than doubled over the last 150 years and on average has grown by nearly 1% per year over the last 40 years [e.g., *Etheridge et al.*, 1998]. This growth rate has slowed over the last 20 years to less than 0.5% per year, and was approximately zero from 1999 through 2002 [*Dlugokencky et al.*, 2003]. At present these changes are not fully understood because of uncertainties in the size, spatial distribution, and trends of CH_4 sources and sinks. Uncertainties in the source strengths can be reduced by measuring the stable carbon isotopic (^{13}C) composition of atmospheric CH_4 since CH_4 source types can be distinguished by their characteristic isotope signatures [e.g., *Bergamaschi et al.*, 2001].

[3] *Allan et al.* [2001a] used the offline transport model TM2 [*Heimann*, 1995] to assess the effects of CH_4 sinks in the extratropical Southern Hemisphere (ETSH; south of 23.5°S). For CH_4, the $^{13}C/^{12}C$ ratio is reported through the $\delta^{13}C$ ratio defined by

$$\delta^{13}C \equiv \left(\left[^{13}CH_4\right]/\left(\left[^{12}CH_4\right] - R_0\right)/R_0, \qquad (1)$$

where $R_0 = (^{13}C/^{12}C)_{PDB}$ has an accepted value of 0.0112372 for the isotope standard, peedee belemnite (PDB) [*Craig*, 1957] and $\delta^{13}C$ is scaled by a factor of 1000, being reported as per mil "‰." *Allan et al.* [2001a] showed that when the change in $\delta^{13}C(CH_4)$ is plotted versus the relative change in mixing ratio (abbreviated from now on to MR) measured in the ETSH over a seasonal cycle, an ellipse-like figure (a "phase ellipse") is obtained. They also showed that the shape of the phase ellipse is modified by source effects, but that the slope of the ellipse major axis appeared to be a robust measure of the kinetic isotope effect (KIE) ε of the oxidation process removing CH_4 from the ETSH lower troposphere. Here $\varepsilon = (k_{13}/k_{12}) - 1$, where k_{13} and k_{12} are the respective rate constants for ^{13}C and ^{12}C removal by the oxidation process. Note that from now on ^{13}C and $\delta^{13}C$ will refer to the carbon in CH_4.

[1] National Institute of Water and Atmospheric Research, Wellington, New Zealand.
[2] National Institute of Water and Atmospheric Research, Lauder, New Zealand.

0148-0227/07/2006JD007369$09.00

[4] *Allan et al.* [2001a] modeled this process using the hydroxyl radical $OH^\bullet$ as the sole oxidant. They found that ε derived from the simulated phase ellipse major axis slope was consistent with the value of ε_{OH} supplied as input to the TM2 model. However, comparison with measurements in New Zealand and Antarctica showed that ε derived from observed ellipses was significantly larger in magnitude than expected for $OH^\bullet$ oxidation alone (−3.9 ‰ [*Saueressig et al.*, 2001]), with a value of about −13 ‰. We refer to this observed ε as ε_A, the "apparent KIE," and ε due to $OH^\bullet$ alone as ε_{OH}. *Allan et al.* [2001b] used a simple chemical box model to demonstrate that a plausible seasonal cycle of chlorine radicals ($Cl^\bullet$) in the marine boundary layer (MBL) acting together with the expected $OH^\bullet$ seasonal cycle could potentially account for the magnitude of ε_A.

[5] *Allan et al.* [2005] fitted sinusoids by nonlinear least squares to both the MR and $\delta^{13}C$ time series between 1991 and 2003 at the observing sites Scott Base, Antarctica (78°S, 167°E), and Baring Head, New Zealand (41°S, 175°E). They found that ε_A was generally much larger in magnitude than ε_{OH}. In 1994–1996 the apparent KIE was about −15 ‰, and in 1998–2000 about −7 ‰. Using a modified version of the simple box model of *Allan et al.* [2001b], they estimated that in an isolated MBL the amplitudes of the $Cl^\bullet$ concentration seasonal cycle required to give the observed effects would be 10^4 atoms cm^{-3} in 1994–1996 and 3×10^3 atoms cm^{-3} in 1998–2000. If the measured enrichment of ^{13}C in CH_4 extends throughout the free troposphere, the seasonal cycle amplitude of $Cl^\bullet$ required in the MBL would be about 6×10^4 $Cl^\bullet$ atoms cm^{-3} in 1994–1996, and about 2×10^4 $Cl^\bullet$ atoms cm^{-3} in 1998–2000. These latter values were based on approximate estimates derived by *Platt et al.* [2004] of the enhancement of $Cl^\bullet$ required in the MBL to account for mixing of ^{13}C-enriched air into the free troposphere. Note that if the 1994–1996 value is taken as an extreme, the seasonal mean $Cl^\bullet$ concentration in 1994–1996 would have been about 3×10^4 $Cl^\bullet$ atoms cm^{-3}. Since the technique can only estimate the magnitude of the seasonal cycle, it is quite possible that the seasonal mean $Cl^\bullet$ concentration in 1998–2000 was not significantly changed, but the seasonal cycle was reduced by some mechanism at present unknown.

[6] In the present work, we employ a much more realistic global circulation model to determine the effects of $Cl^\bullet$ in the model MBL on the MR and $\delta^{13}C$ of CH_4 introduced into the model atmosphere by plausible CH_4 sources and sinks. We show that the simulated seasonal cycles of MR and $\delta^{13}C$ are realistic, and from these we infer values for the apparent KIE in a range of scenarios including different levels of $Cl^\bullet$ in the MBL. We then determine the $Cl^\bullet$ concentrations required in the MBL to produce the apparent KIE values observed at ETSH sites by *Allan et al.* [2005]. From these we estimate the likely size of the global $Cl^\bullet$ sink for CH_4 required to give the observed apparent KIE values.

2. Model Description

[7] We use a modification of the U.K. Met Office's Unified Model (UM) [*Cullen and Davies*, 1991], a general circulation model employed for weather forecasting and climate prediction in the U.K. and elsewhere, which we will refer to as UMeth (Unified Model with Methane). UMeth includes the surface emission, atmospheric transport and in situ destruction of CH_4. We use version 4.5 of the UM, which assumes a hydrostatic atmosphere. The model was configured with a horizontal resolution of 2.5° (latitude) and 3.75° (longitude), with 19 vertical levels [*Pole et al.*, 2000]. Table 1 shows the mean pressures and approximate altitudes of the first 5 levels, which encompass the important MBL region. The UM includes a parameterization of turbulent boundary layer mixing of tracers that is based on a first-order turbulent closure approximation. The amount of mixing depends on the local wind shear and atmospheric stability and therefore is greatest in the tropics. Simple idealized tests indicate that the turbulent boundary layer mixing timescales are of the order of two hours or less and vary by a factor of two from the poles to the equator. Turnover between the MBL and the free troposphere occurs on a timescale of several days.

[8] The transport of long-lived atmospheric trace gases in the UM was studied by *Gregory and West* [2002]. They showed that the default flux-limited total-variation-diminishing (TVD) tracer advection scheme used in the UM gave unrealistic "stratospheric tape recorder" effects. They also evaluated the performance of advection schemes based on the NIRVANA (Nonoscillatory Integrally Reconstructed Volume-Averaged Numerical Advection) scheme of *Leonard et al.* [1995]. They found that use of an extended NIRVANA scheme with monotonic quintic interpolation significantly improved the UM's advection of water vapor in the stratosphere and its tape recorder properties. We evaluated the TVD scheme and *Gregory and West*'s [2002] extended NIRVANA scheme in the UM configuration used in the present work (H. Struthers et al., A comparison of the transport of long-lived atmospheric trace gas species from two advection schemes incorporated into an atmospheric general circulation model, submitted to *Tellus*, 2006). The resulting vertical distributions of both CH_4 and $\delta^{13}C$ in the stratosphere were much more realistic using the extended NIRVANA scheme than using the standard TVD scheme. We therefore apply the extended NIRVANA scheme in UMeth to transport the two methane isotopic species ($^{12}CH_4$ and $^{13}CH_4$), which are chemically destroyed via reaction with an $OH^\bullet$ climatology based on *Houweling et al.* [1998]. This climatology gives a global mean tropospheric $OH^\bullet$ concentration of 1.08×10^6 molecules cm^{-3}, similar to the value 1.16×10^6 molecules cm^{-3} derived by *Spivakovsky et al.* [2000].

[9] We include surface CH_4 sources, the above $OH^\bullet$ climatology, the 30 Tg y^{-1} integrated stratospheric sink, and the 38 Tg y^{-1} soil sink from the International Geosphere-Biosphere Program Global Atmospheric Methane Synthesis scenario (GAMeS) (S. Houweling, personal communication, 2001). The source strengths and $\delta^{13}C$ values are shown in Table 2. $OH^\bullet$ concentrations are interpolated in time from the monthly GAMeS climatology. CH_4 is oxidized by $OH^\bullet$ at each time step of the model. The reaction rate constant for the CH_4 oxidation is taken from *Sander et al.* [2003]:

$$k = 2.45 \times 10^{-12} \exp(-1775/T) \quad (2)$$

where T is absolute temperature and k is in units of cm^3 $molecule^{-1}$ s^{-1}.

Table 1. MBL Model Level Pressures and Altitudes Calculated Using Averaged Surface Pressure, Surface Temperature, and Atmospheric Temperatures Over the Last 16 Years of the Model Run[a]

Model Level	Nominal Pressure, hPa	Nominal Altitude, m
1	1007.43	25
2	985.16	214
3	940.15	604
4	878.93	1162
5	800.47	1927

[a]The values are global means (latitudinal weighting) of all open ocean grid points. Levels 4 and 5 may often be in the free troposphere.

[10] Although the GAMeS scenario is not optimized for estimated 2006 CH_4 emissions, it is a convenient resource for our application of the UM, in which we do not "nudge" toward the dynamics of any specific real year and therefore do not need the most recent CH_4 budgets. The CH_4 sources (biomass burning, rice cultivation, termites, bogs, swamps, coal, oil, gas, animals and landfills) are specified in kg m^{-2} s^{-1} at each horizontal grid point of the model, as is a soil sink specified as a negative source in kg m^{-2} s^{-1}. The biomass burning, rice, bogs, and swamps sources and the soil sink vary on a monthly basis, with the same annual cycle of sources being repeated each year of the model integration. The other sources are constant. The total annual CH_4 source is 580 Tg y^{-1}. The constant $\delta^{13}C$ values for the sources are assigned as specified in the GAMeS scenario, with a weighted mean source $\delta^{13}C$ of −51.5 ‰. The $OH^\bullet$ KIE is taken to be $\varepsilon_{OH} = -3.9$ ‰. [*Saueressig et al.*, 2001].

[11] UMeth was initialized using equilibrated $^{12}CH_4$ and $^{13}CH_4$ fields from a previous version of the model. For all the experiments discussed in this paper, the model was run for 40 years allowing achievement of a steady state where the sources and sinks of CH_4 are balanced apart from small seasonal variations (see Figure 2).

[12] We drove UMeth with the composite 4-year El Niño and La Niña sea surface temperature (SST) cycle developed by *Spencer et al.* [2004]. *Spencer and Slingo* [2003] showed that the UM's atmospheric response to a composite of 5 El Niño and 5 La Niña events compares well with National Centers for Environmental Prediction/National Center for Atmospheric Research reanalysis data, particularly in the tropics. *Allan et al.* [2005] demonstrated using an earlier version of UMeth with a single atmospheric CH_4 sink ($OH^\bullet$) that the large magnitudes of apparent KIE values measured at Baring Head and Scott Base are very unlikely to arise from El Niño Southern Oscillation (ENSO) transport effects.

[13] The temporal and spatial variations of $Cl^\bullet$ in the MBL are essentially unknown. However, by applying a simple scenario of specified $Cl^\bullet$ atom concentrations in the MBL of UMeth, we can gain insight into the effects of temporal and spatial variations of the MBL $Cl^\bullet$ sink. The structure shown in Figure 1 is derived from the function

$$Cl^\bullet = Cl^\bullet_{mean} + Cl^\bullet_P \tanh(3\lambda)\sin(2\pi(t-90)/365), \qquad (3)$$

where time t is in days and λ is latitude in radians. Since the evolution of $Cl^\bullet$ in the MBL appears to be a photolytic process [e.g., *Allan et al.*, 2005], the time dependence assumes a sinusoidal seasonal cycle with a maximum at 1 January in the Southern Hemisphere, close to the summer solstice (and a minimum in the Northern Hemisphere at the same time). The $\tanh(3\lambda)$ term makes the $Cl^\bullet$ seasonal cycle amplitude decrease slowly toward the equator outside the tropics, and then change rapidly through zero as the equator is traversed. This behavior represents the seasonal change of solar illumination at each latitude, and is chosen to give midwinter $Cl^\bullet$ concentrations of a few hundred atoms cm^{-3} at latitude 40° S, consistent with recent simulations (R. von Glasow, personal communication, 2006). The adjustable constants $Cl^\bullet_{mean}$ and $Cl^\bullet_P$ are respectively the seasonal mean and the seasonal sinusoid amplitude at the poles. Note that $Cl^\bullet_{mean}$ is constant everywhere, and the full second term in (3) represents the latitudinal variation of the seasonal cycle. In Figure 1, $Cl^\bullet_{mean} = Cl^\bullet_P = 10^4$ atoms cm^{-3}. Function (3) is applied only at MBL grid cells containing open ocean surface, with land and sea ice areas excluded. It is also applied only at grid cells below 900 m altitude, representing the region in which the MBL typically occurs in UMeth. Note that we do not include diurnal variations of $Cl^\bullet$. Also, the trough-to-peak amplitude, $\Delta Cl^\bullet$, of the $Cl^\bullet$ seasonal cycle [*Allan et al.*, 2005] is given here by $\Delta Cl^\bullet = 2\ Cl^\bullet_P\ |\tanh(3\lambda)|$.

[14] The constant value with latitude for $Cl^\bullet_{mean}$ was chosen as the simplest case. It is possible, for example, that $Cl^\bullet_{mean}$ increases from the poles to the equator, although there is no observational evidence for this at present. This would not significantly affect the ε_A values derived in this work, but would mean that the global $Cl^\bullet$ sink for CH_4 would be larger than we obtain in section 4. It is also possible that winter minimum values of $Cl^\bullet$ in the extratropical regions are larger than the few hundred atoms cm^{-3} that we assume. Again, this would not affect our derived ε_A values, but would lead to a larger global $Cl^\bullet$ sink. Thus our choice of constant $Cl^\bullet_{mean}$ may well be conservative in terms of deriving the magnitude of the global $Cl^\bullet$ sink for CH_4.

[15] We have assumed in the above that the evolution of $Cl^\bullet$ in the MBL is related to heterogeneous chemistry probably involving the oxidation of dimethylsulfide (DMS) and the subsequent acidification of sea salt droplets, as

Table 2. Source Strengths and $\delta^{13}C$ Values From the GAMeS Scenario

Source	Source Strength, Tg yr^{-1}	$\delta^{13}C$, ‰	Monthly Varying
Animals	98.0	−62.0	no
Biomass burning	49.4	−25.0	yes
Bogs	40.3	−64.3	yes
Coal	41.7	−35.2	no
Gas	48.0	−40.2	no
Landfills	47.7	−51.1	no
Oil	34.5	−40.1	no
Rice cultivation	80.0	−62.7	yes
Swamps	121.7	−54.8	yes
Termites	19.3	−57.0	no
Soil sink	−37.9	−69.0	yes
Total emissions excluding soil sink	580.6		

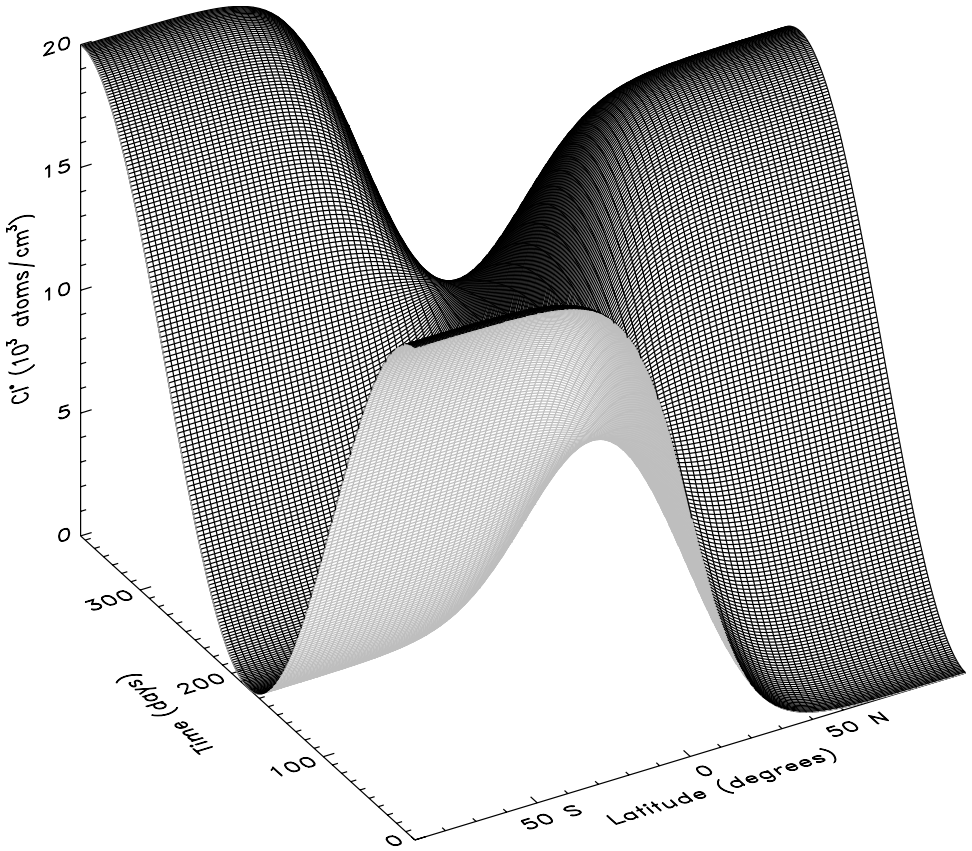

Figure 1. Functional form of assumed $Cl^{\bullet}$ sink structure in latitude and time. The function shown has constant $Cl^{\bullet}_{mean} = 10^4$ atoms cm^{-3}. It is applied only where there is open ocean.

discussed by *Allan et al.* [2001b, 2005] following *Vogt et al.* [1996]. The details of this are very complex, and we are currently attempting to clarify the process using a model of heterogeneous chemistry in the MBL (R. von Glasow, personal communication, 2006).

[16] Oxidation of CH_4 by $Cl^{\bullet}$ within the model is treated in an analogous manner to oxidation by $OH^{\bullet}$. The rate constant for the $CH_4 + Cl^{\bullet}$ reaction is [*Sander et al.*, 2003]

$$k = 9.6 \times 10^{-12} \exp(-1360/T). \quad (4)$$

where again T is absolute temperature and k is in units of cm^3 $molecule^{-1}$ s^{-1}.

[17] The temperature dependence of the KIE for this reaction [*Saueressig et al.*, 1995] is included as

$$KIE_{Cl} = 1.043 \exp(6.455/T). \quad (5)$$

This gives a KIE of between 1.065 and 1.068 for typical temperatures within the MBL.

3. Simulation Results

[18] We ran UMeth for a number of 4-year ENSO cycles with a range of values of $Cl^{\bullet}_{mean}$, applying $Cl^{\bullet}_{P} = Cl^{\bullet}_{mean}$ in each case. The range was $Cl^{\bullet}_{mean} = \{0, 1, 3, 6, 10, 14, 18, 22, 26, 30\} \times 10^5$ atoms cm^{-3}. The results for globally integrated atmospheric quantities are given in Figure 2. Figure 2a shows the sum of the integrated $^{12}CH_4$ and $^{13}CH_4$ masses for all runs, while Figure 2b shows the corresponding $\delta^{13}C$ derived using (1) from the integrated $^{12}CH_4$ and $^{13}CH_4$ masses. All runs have reached approximate steady state as measured by constant mean CH_4 mass and $\delta^{13}C$ over the last few ENSO cycles. As expected, the global CH_4 mass decreases as $Cl^{\bullet}_{mean}$ increases, and $\delta^{13}C$ becomes more positive as $Cl^{\bullet}_{mean}$ increases. The 4-year ENSO cycles are apparent in Figure 2a as modulations of the seasonal cycle amplitudes over consecutive 4-year periods. They are not seen in Figure 2b as the ratio in (1) eliminates them. The seasonal cycle amplitudes in Figure 2b increase significantly as $Cl^{\bullet}_{mean}$ increases from 0 to 30×10^3 atoms cm^{-3}. Quantitative results from these global values will be discussed in section 4. However, in section 3.1 we consider the results for $Cl^{\bullet}_{mean} = 0$ in detail as a baseline for comparison with the results for nonzero $Cl^{\bullet}_{mean}$ described in section 3.2.

3.1. Excluding $Cl^{\bullet}$ Sink

[19] In Figure 2a for $Cl^{\bullet}_{mean} = 0$, the final atmospheric CH_4 burden, averaged over the last 8 years of the integration, is 4965 Tg. From this we infer the tropospheric CH_4 turnover time against OH loss to be 9.6 years, with a whole atmosphere turnover time of 8.5 years. Both are consistent with Intergovernmental Panel on Climate Change estimates [*Prather et al.*, 2001].

[20] We applied the sinusoidal least squares fitting approach described in section 1 to the MR and $\delta^{13}C$ UMeth output for each of the final 8 years of the simulation

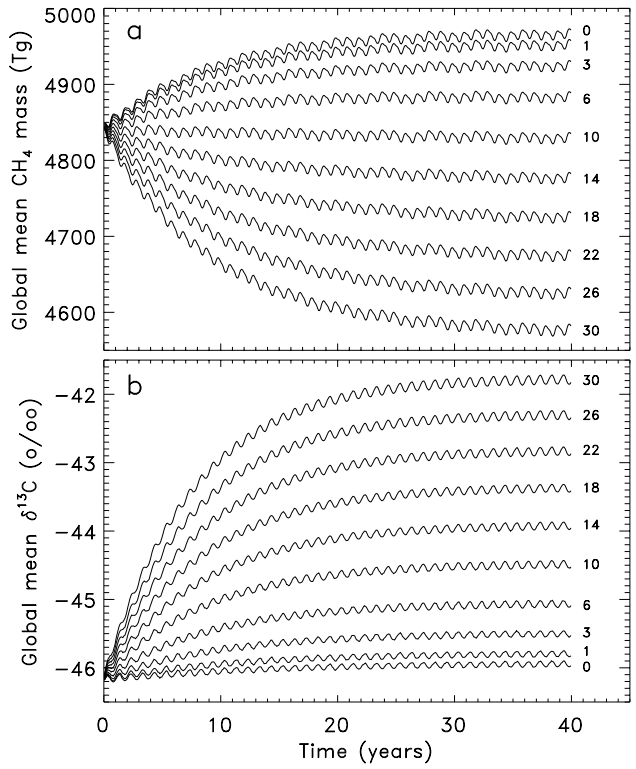

Figure 2. (a) Integrated global CH_4 mass for the range of UMeth simulations carried out. The curves are labeled with the appropriate value of $Cl^{\bullet}_{mean}$ in units of 10^3 atoms cm^{-3}. (b) Corresponding curves for global $\delta^{13}C$.

(covering 2 ENSO cycles) at the cell containing the Baring Head site. Figures 3a and 3c show the results of this fitting process for Year 2 of the final 8 years. Table 3 shows the estimates we obtained of the apparent KIE, ε_A, where the errors are uncertainties in the least squares fits. There is no significant difference between these estimates, and no significant dependence on the ENSO cycle. Because of this lack of ENSO dependence, we are able to treat the ε_A values from each year as independent estimates. We then combine the 8 values weighted by the individual uncertainties of the least squares fits into an overall mean that we quote with a 2σ uncertainty. The overall weighted mean is -3.85 ± 0.08 ‰ (2σ), which is a good estimate of the input KIE $\varepsilon_{OH} = -3.9$ ‰. All 8-year means from now on follow this procedure.

[21] These results show that (1) the KIE for a single atmospheric sink can be derived using the MR/$\delta^{13}C$ technique from a completely different transport model to the TM2 offline model and (2) changing transport effects during the composite ENSO cycle do not significantly affect the derived KIE. However, we note that the corresponding results for Scott Base are slightly different. Figures 4a and 4c show that the UMeth output at Scott Base has less variability than at Baring Head, a property also noted for the TM2 model by *Allan et al.* [2001a]. The overall weighted mean of the final 8 years at Scott Base is -4.23 ± 0.04 ‰ (2σ). We show in section 3.2 that there is a systematic difference between ε_A derived at Baring Head and Scott Base. This difference for $Cl^{\bullet}_{mean} = 0$ is still very small compared with the difference between $\varepsilon_{OH} = -3.9$ ‰ and the measured ε_A at these stations.

[22] We are therefore confident that the measured variations of the apparent KIE shown in Figure 4 of *Allan et al.* [2005] do not arise from spurious variations in the apparent KIE for the $OH^{\bullet}$ sink, and so most likely relate to a CH_4 sink mechanism additional to $OH^{\bullet}$.

3.2. Including $Cl^{\bullet}$ Sink

[23] We now hypothesize that the additional sink mechanism is provided by significant amounts of $Cl^{\bullet}$ in the MBL, and we attempt in section 4 to estimate the MBL concentration of $Cl^{\bullet}$ required to match observational estimates of ε_A.

[24] Figures 3b and 3d show the MR and $\delta^{13}C$ cycles for Year 2 of the final 8 years with $Cl^{\bullet}_{mean} = 22 \times 10^3$ atoms cm^{-3}. The MR cycle amplitude is only slightly increased from that in Figure 3a for $Cl^{\bullet}_{mean} = 0$, but the $\delta^{13}C$ cycle amplitude in Figure 3d is much larger than that in Figure 3c. The fitted sinusoidal amplitudes give $\varepsilon_A = -13.06 \pm 0.35$ ‰ when $Cl^{\bullet}_{mean} = 22 \times 10^3$ atoms cm^{-3}. This shows that a significant concentration of $Cl^{\bullet}$ in the MBL is able to reproduce apparent KIE values consistent with those derived from observations at the same position. The corresponding UMeth results for Scott Base are shown in Figures 4b and 4d. These give $\varepsilon_A = -13.96 \pm 0.24$ ‰, again a small systematic difference from the Baring Head value.

[25] We now combine ε_A values for the final 8 years of each $Cl^{\bullet}$ simulation into weighted means as discussed in section 3.1. The results are shown in Figure 5a for Baring Head and Scott Base, the "error" bars representing 2σ uncertainties. A consistent increase in the magnitude of ε_A with $Cl^{\bullet}_{mean}$ can be seen, with Scott Base values systematically about 10% larger in magnitude than Baring Head values. Figure 5b shows corresponding weighted means of the phase differences $\Delta\varphi$ between the MR and $\delta^{13}C$ fitted sinusoids. Again there is a systematic difference between Baring Head and Scott Base, but both tend asymptotically to π as $Cl^{\bullet}_{mean}$ increases. The significance of this is discussed in section 4.

4. Discussion

[26] In Figures 3 and 4 there is noticeable variability from day to day in the UMeth output. This is possibly a result of small-scale transport effects bringing incompletely mixed air to the local grid cell. The smaller variability at Scott Base compared with Baring Head could be interpreted as resulting from smaller spatial gradients in $^{12}CH_4$ and $^{13}CH_4$ near Antarctica. However, both at Baring Head and Scott Base, there is larger variability in the 3 months after 1 January for the $\delta^{13}C$ cycles when $Cl^{\bullet}_{mean} = 22 \times 10^3$ atoms cm^{-3}. This is generally the case when $Cl^{\bullet}_{mean}$ is nonzero. One interpretation could be that the existence of $Cl^{\bullet}$ in the MBL produces $^{13}CH_4$ enriched air that is intermittently released from the MBL at different times and positions, and is then carried to the local grid cell. Further work is required to test these suggestions.

[27] The $\delta^{13}C$ cycle at Scott Base in Figure 4d is slightly distorted compared with that at Baring Head in Figure 3d. This could lead to a slight overestimate of the $\delta^{13}C$ cycle amplitude near Antarctica, and could possibly explain the

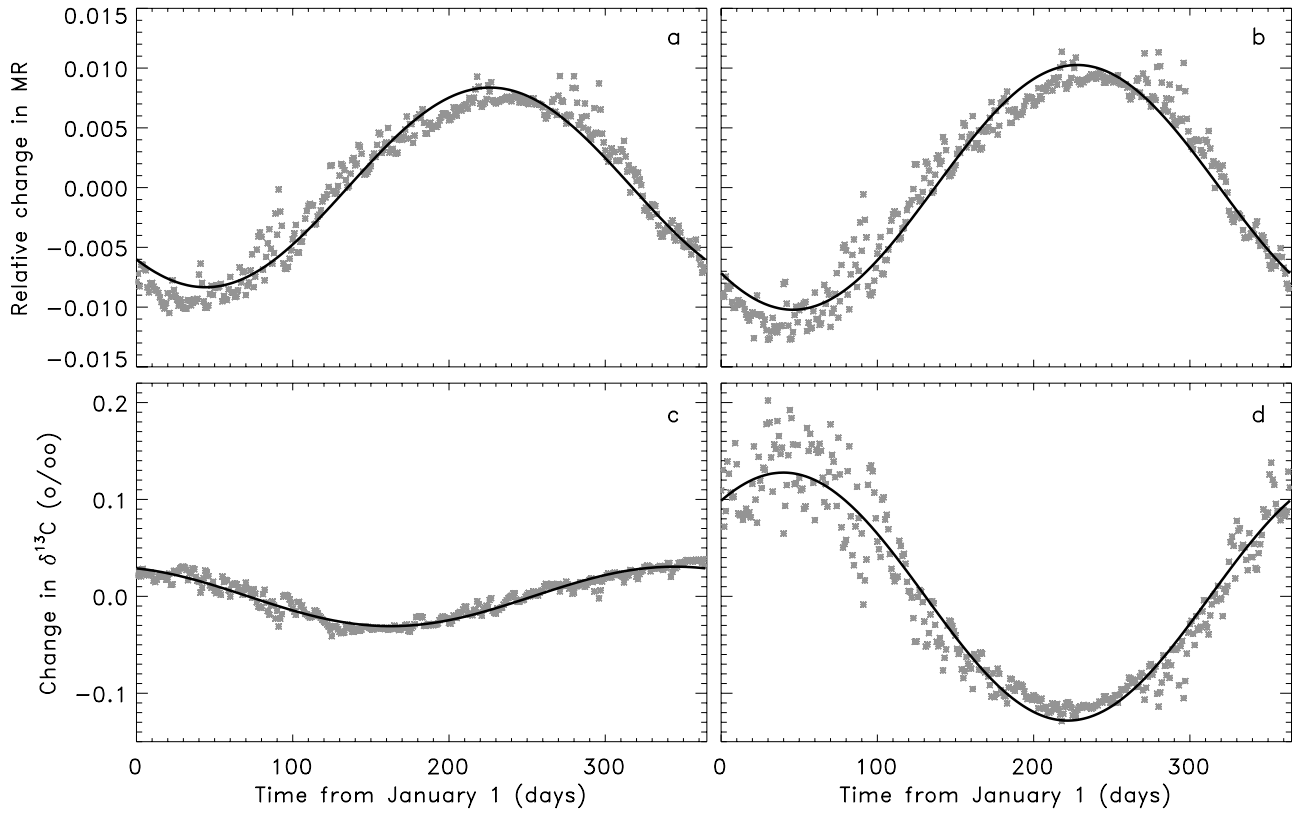

Figure 3. UMeth output: daily means (grey asterisks) at Baring Head of the relative change in MR for (a) $Cl^{\bullet}_{mean} = 0$ and (b) $Cl^{\bullet}_{mean} = 22 \times 10^3$ atoms cm^{-3}, for year 2 of the final 8 years. (c and d) Corresponding $\delta^{13}C$ values. The solid curves are sinusoids fitted by nonlinear least squares.

systematic difference between the Scott Base and Baring Head values in Figure 5a. We considered the possibility that seasonal differences in cross tropopause transport over Antarctica could create this difference by allowing enriched stratospheric air to reach Antarctica at some times of the year. To test this, we ran UMeth with the stratospheric sink switched off, but found no significant effect on the $\delta^{13}C$ cycles. This null result is supported by the fact that such transport of enriched air should give the same absolute difference between Scott Base and Baring Head for all the points in Figure 5a, while there is actually a 10% relative difference between the sites. Whichever way this difference arises, we consider that the accurate value for ε_{OH} derived at Baring Head suggests that the most reliable estimates of ε_A for nonzero $Cl^{\bullet}_{mean}$ are likely to be obtained from seasonal cycles simulated at ETSH midlatitudes. We therefore consider only the Baring Head curve in Figure 5a from now on.

[28] The observational results presented by *Allan et al.* [2005] suggest that ε_A was about −15 ‰ in 1994–1996, and about −7 ‰ in 1998–2000. From Figure 5a, these imply $Cl^{\bullet}_{mean}$ values of about 28×10^3 atoms cm^{-3} in 1994–1996 and about 9×10^3 atoms cm^{-3} in 1998–2000. These values are very close to the corresponding values suggested by *Allan et al.* [2005] using results from a simple chemical box model of the MBL scaled by an effective tropospheric height as described by *Platt et al.* [2004]. The question then arises as to how the global (or at least hemispheric) MBL $Cl^{\bullet}$ concentration could change by such a large factor over a few years. This would require either the summer maximum $Cl^{\bullet}$ concentration to decrease significantly, or the winter minimum $Cl^{\bullet}$ concentration to increase significantly, or a combination of the two. Any such process that reduces the $Cl^{\bullet}$ seasonal cycle amplitude would give the same observational result, as our method of determining ε_A is sensitive only to that amplitude. The value of $Cl^{\bullet}_{mean}$ would be different in each case, but at present we have no way of determining this. Direct measurements of $Cl^{\bullet}$ seasonal cycles in the MBL would be required, or failing that, the use of detailed MBL chemical process models. *Wingenter et al.* [2005] reported an inferred morning average $Cl^{\bullet}$ concentration in the MBL near Christmas Island (2°N, 157°W) of about 70×10^3 atoms cm^{-3}. This implies a 24-hour average concentration of at least $20–30 \times 10^3$ atoms cm^{-3}, comparable with our estimated

Table 3. Apparent KIE Values at Baring Head for the Final 8 Years of the Simulation With $Cl^{\bullet}$ Excluded[a]

Year	Apparent KIE, ‰	ENSO Phase
1	−3.84 ± 0.14	El Niño
2	−3.85 ± 0.10	El Niño
3	−3.69 ± 0.12	La Niña
4	−3.81 ± 0.12	La Niña
5	−4.08 ± 0.12	El Niño
6	−3.86 ± 0.12	El Niño
7	−3.81 ± 0.10	La Niña
8	−3.90 ± 0.15	La Niña

[a]The errors are derived from the sinusoidal fits.

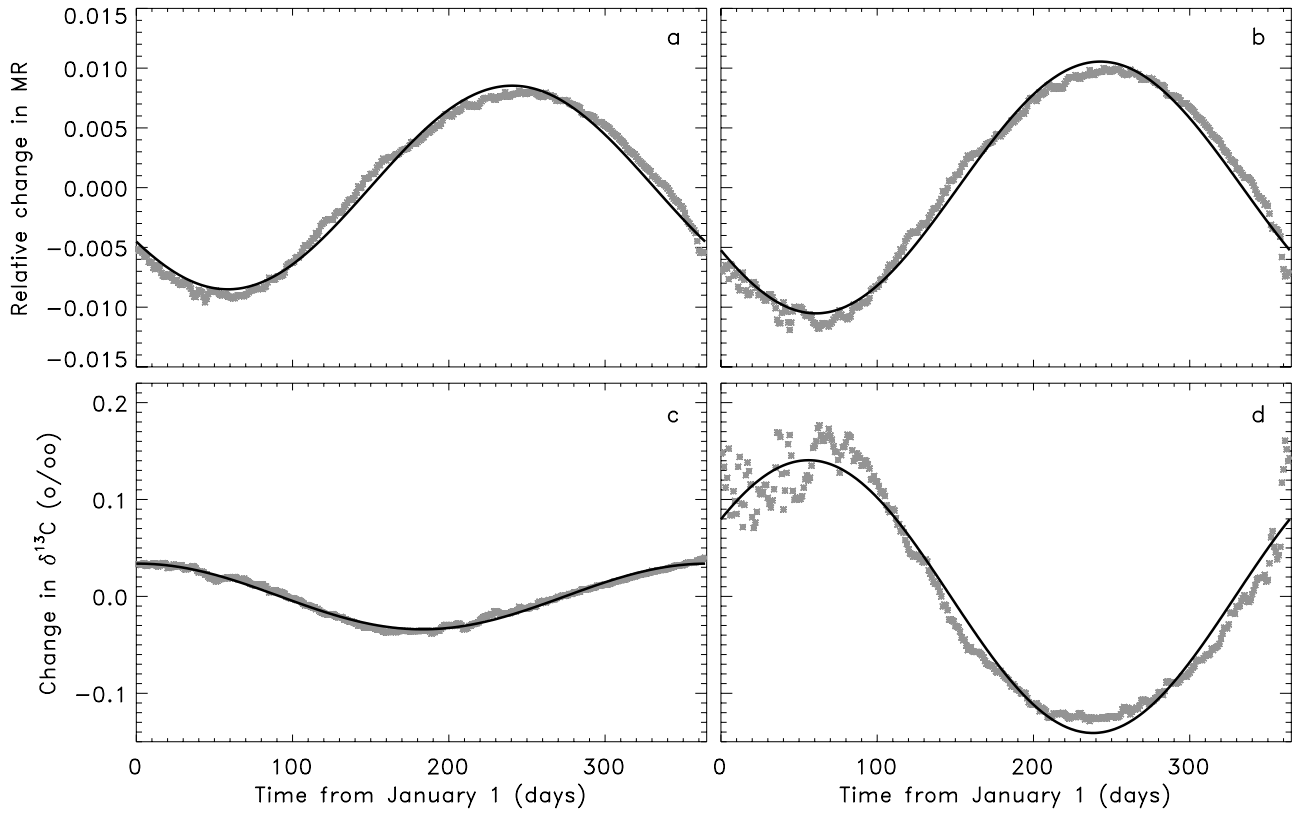

Figure 4. (a–d) As Figure 3 for Scott Base.

$Cl^{\bullet}_{mean}$ value. Similar $Cl^{\bullet}$ concentrations were inferred by *Wingenter et al.* [1996] in the North Atlantic, east of the Azores. In the following, we take the inferred value of 9×10^3 atoms cm^{-3} in 1998–2000 as a conservative lower bound on the mean MBL $Cl^{\bullet}$ concentration in that period.

[29] It is of interest to look at the global properties of the MBL $Cl^{\bullet}$ sink. The sink strength for our chosen spatial and temporal sink structure can be obtained in a straightforward manner from the rate equation for the total atmospheric CH_4 burden *B*. The result is

$$S_{Cl} = S_0[1 - (B_{X+Cl}/B_X)], \quad (6)$$

where S_{Cl} is the MBL $Cl^{\bullet}$ sink strength, S_0 is the total sink strength (equal to the total source strength at steady state), B_X is the total atmospheric CH_4 burden at steady state when the $Cl^{\bullet}$ sink is excluded, and B_{X+Cl} is the corresponding quantity when the $Cl^{\bullet}$ sink is included. The required values of *B* can be obtained from Figure 2a, and the resulting $Cl^{\bullet}$ sink strengths are shown versus $Cl^{\bullet}_{mean}$ by the full line in Figure 6a. The implied $Cl^{\bullet}$ sink strengths are about 37 Tg y^{-1} in 1994–1996 and about 13 Tg y^{-1} in 1998–2000 for our conservative lower bound, with a mean value of 25 Tg y^{-1}. The global change in δ^{13}C engendered by our range of $Cl^{\bullet}_{mean}$ values is shown by the dashed line in Figure 6a. A $Cl^{\bullet}$ sink strength of 25 ± 12 Tg y^{-1} would imply a global enrichment of δ^{13}C by 2.6 ± 1.2 ‰. Neither a MBL $Cl^{\bullet}$ sink of strength 25 ± 12 Tg y^{-1} nor the corresponding 2.6 ± 1.2 ‰ atmospheric enrichment have yet been taken account of in global CH_4 budgets. Note also that this $Cl^{\bullet}$ sink would lead to a 0.4 ± 0.2 year reduction in CH_4 turnover time unless it was compensated for by reductions in other sinks.

[30] In this context, recent measurements [*Keppler et al.*, 2006] of a vegetation source of CH_4 are of interest. *Keppler et al.* [2006] estimated this vegetation source strength to be 62–236 Tg y^{-1}, values that would require a large revision of the current global methane budget. However, recent studies have suggested that the actual vegetation emissions may be much smaller than suggested by *Keppler et al.* [2006]. For example, *Ferretti et al.* [2007] suggested from comparisons with recent ice core measurements that the vegetation source may only be 0–46 Tg y^{-1}. *Kirschbaum et al.* [2006] suggested a range of 10–60 Tg y^{-1} using different assumptions to upscale *Keppler et al.*'s [2006] measurements to a global vegetation source strength. If these values prove to be correct, the vegetation CH_4 source may only be of the order of 30 Tg y^{-1}. This is similar in magnitude to our derived value for the MBL $Cl^{\bullet}$ sink strength. Therefore it may turn out that inclusion of both the new vegetation source and $Cl^{\bullet}$ sink in the global methane budget would not change that budget in gross terms, only in detail. However, recent work by *Houweling et al.* [2006] used a model/data comparison to estimate a plausible upper bound of 85 Tg y^{-1} for vegetation emissions.

[31] *Keppler et al.* [2006] estimated that the vegetation CH_4 source could have a δ^{13}C of about −50 ‰. This is close to the generally quoted mean global source δ^{13}C, and so the vegetation source would impact on the global ^{13}C budget only if it partly replaced sources with significantly different δ^{13}C values, such as wetlands and rice sources

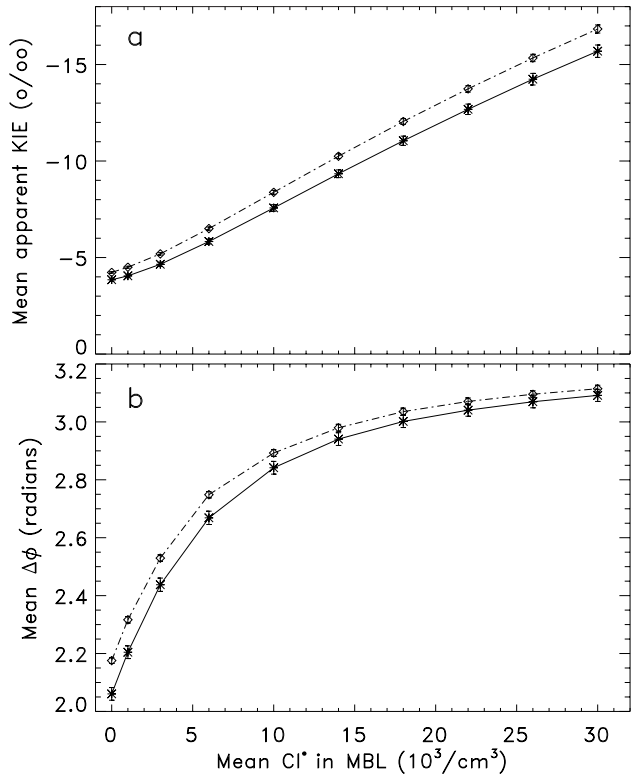

Figure 5. (a) Mean apparent KIE ε_A inferred from MR and $\delta^{13}C$ seasonal cycles at Baring Head (solid line) and Scott Base (dash-dotted line) versus $Cl^{\bullet}_{mean}$. (b) Mean phase difference $\Delta\phi$ between MR and $\delta^{13}C$ seasonal cycles at Baring Head (solid line) and Scott Base (dash-dotted line).

[*Houweling et al.*, 2006]. As discussed above, we estimate our 25 Tg y^{-1} $Cl^{\bullet}$ sink would enrich the global atmosphere by 2.6 ‰. This sink should be included in global methane budgets, as even a small sink strength has a relatively large isotopic effect. Aspects of this are discussed in more detail by *Lassey et al.* [2006]. *Houweling et al.* [2006] did not consider the effect of a MBL $Cl^{\bullet}$ sink in their estimate of the vegetation source strength. There is clearly much work to be done on clarifying the global methane budget.

[32] It should be carefully noted that the ε_A values given in Figure 5a for nonzero $Cl^{\bullet}_{mean}$ are not the effective ε values for the combined tropospheric $OH^{\bullet}$ + $Cl^{\bullet}$ sink (ε_{OH+Cl}) responsible for the global atmospheric enrichment mentioned above. The value of ε_{OH+Cl} is given by the mean of ε_{OH} and ε_{Cl} weighted by the strengths of the individual $OH^{\bullet}$ and $Cl^{\bullet}$ sinks. For example, when the MBL $Cl^{\bullet}$ sink strength is 25 Tg y^{-1}, the tropospheric $OH^{\bullet}$ sink strength is 488 Tg y^{-1}. The weighted mean ε_{OH+Cl} is then −6.9 ‰, much less than the ε_A value of −11.1 ‰ for the 25 Tg y^{-1} $Cl^{\bullet}$ sink. Applying equation (6) of *Allan et al.* [2001a] with ε_{OH+Cl} = −6.9 ‰, the 25 Tg y^{-1} $Cl^{\bullet}$ sink enriches the atmosphere by 2.6 ‰, as found in the UMeth results. Thus ε_A is the link between the Baring Head measurements and the equivalent simulated results in UMeth that allows us to determine the $Cl^{\bullet}$ sink strength, but it is not a direct measurement of ε_{OH+Cl}. The relationship between the global ε_{OH+Cl} and ε_A at Baring Head is shown in Figure 6b.

[33] An interesting point is the change in $\Delta\varphi$ shown in Figure 5b as $Cl^{\bullet}_{mean}$ increases. *Allan et al.* [2001a] showed that $\Delta\varphi$ increased as the biomass burning source in the TM2 model was increased. Therefore they interpreted changes in $\Delta\varphi$ as being dominantly caused by changes in seasonally varying sources. They included a specified $OH^{\bullet}$ sink in their model, as we have in UMeth. However, our ability to vary the strength of the MBL $Cl^{\bullet}$ sink shows that changes in $\Delta\varphi$ have more complex causes. Our interpretation of the variation in Figure 5b is that a local sink tries to pull $\Delta\varphi$ toward the value π that would occur if the sink were completely isolated from seasonal source effects. We infer that external seasonal sources are imposing a significant phase shift away from π in Figure 5b, but (for $Cl^{\bullet}_{mean}$ = 0) the local $OH^{\bullet}$ sink has already moved $\Delta\varphi$ toward π. As $Cl^{\bullet}_{mean}$ increases, the total local sink effect begins to dominate, and $\Delta\varphi$ moves very close to π. Therefore the closeness of $\Delta\varphi$ to π is a measure of how dominant local sink effects are over external seasonal source effects. The difference in $\Delta\varphi$ between Scott Base and Baring Head could be an effect of the distortion of the $\delta^{13}C$ cycle at Scott Base discussed earlier in this section, but it could also be a result of Scott Base lying further away from seasonal source effects than Baring Head.

[34] Note that *Allan et al.* [2001a] quoted a mean value of 2.53 radians for $\Delta\varphi$ observed at Baring Head over the period 1993–1996. Taken at face value, this would seem to imply a smaller value for $Cl^{\bullet}_{mean}$ than we deduce from the corresponding seasonal cycle amplitude measurements.

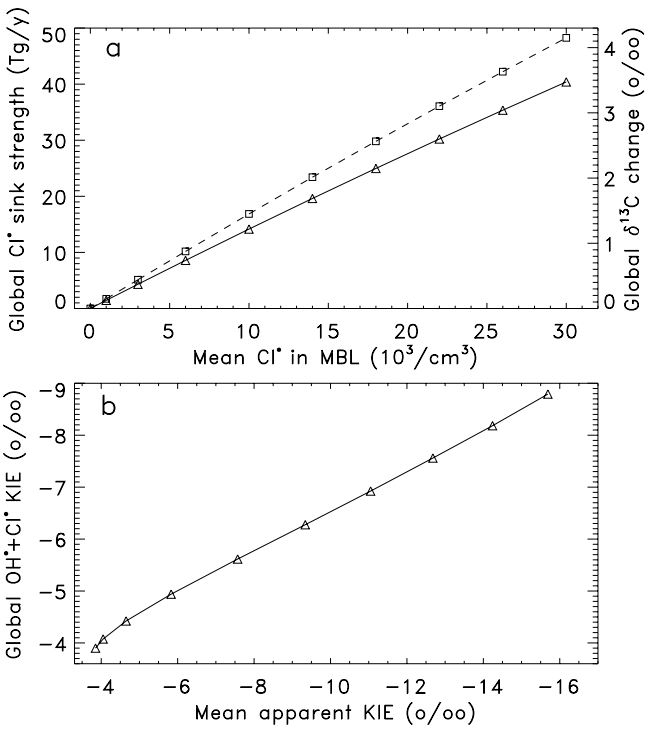

Figure 6. (a) Global $Cl^{\bullet}$ sink strength for CH_4 (solid line) and global $\delta^{13}C$ change (dashed line) versus $Cl^{\bullet}_{mean}$. (b) Global $OH^{\bullet}$ + $Cl^{\bullet}$ combined sink KIE versus simulated apparent KIE inferred at Baring Head.

However, $\Delta\varphi$ is affected by the choice of magnitude and time dependence of seasonally varying sources, seasonality of cross-equatorial transport, and small differences in the times of seasonal maxima of the $OH^\bullet$ and $Cl^\bullet$ sinks. Work is in progress to quantify these effects on $\Delta\varphi$.

[35] A related point concerns the MR and $\delta^{13}C$ cycles measured by *Morimoto et al.* [2006] at Ny Ålesund, Svalbard (79° N, 12° E). If we were to assume that these cycles arise from an atmospheric sink effect, a rough estimate of the amplitudes of the measured cycles gives an apparent ε_A value with average magnitude about 15 ‰. When we examine the cell including Ny Ålesund in our UMeth simulation with $Cl^\bullet_{mean} = 0$, we find erratic MR and $\delta^{13}C$ cycles with average apparent ε_A magnitudes of about 15 ‰. The true atmospheric sink ε_A in this simulation was −3.9 ‰. Therefore the large apparent ε_A at Ny Ålesund in both the measurements and the simulation must arise from source effects. We therefore agree with *Morimoto et al.* [2006] that their observations at Ny Ålesund are dominated by source effects. It appears from our UMeth results that ETSH midlatitudes are the regions where source effects are minimized and ε_A can be determined most accurately.

5. Conclusions

[36] We have presented simulation results from UMeth, a general circulation model incorporating CH_4 emission, transport, and destruction by sinks including a specified $Cl^\bullet$ sink in the MBL of the model. This sink has a structure with large seasonal cycles in the extratropical regions, and a constant mean value of $Cl^\bullet$ concentration ($Cl^\bullet_{mean}$) in the MBL in regions of open ocean.

[37] For $Cl^\bullet_{mean} = 0$, the results show that an accurate value for ε_{OH}, the KIE due to the $OH^\bullet$ sink, can be obtained from the amplitudes of the MR and $\delta^{13}C$ seasonal cycles at the Baring Head station in ETSH midlatitudes. The corresponding value derived at Scott Base in Antarctica is about 10% too large in magnitude, possibly because of distortion of the $\delta^{13}C$ seasonal cycle there.

[38] For nonzero $Cl^\bullet_{mean}$, there is a consistent increase in the amplitudes of the $\delta^{13}C$ seasonal cycles as $Cl^\bullet_{mean}$ increases, giving a corresponding increase in the apparent KIE ε_A. The derived values of ε_A at Scott Base are consistently about 10% larger than at Baring Head. Because Baring Head gives an accurate estimate of ε_{OH}, we assume that the simulated Baring Head values of ε_A also give good estimates of the ε_A values associated with the composite $OH^\bullet + Cl^\bullet$ sink for comparison with the equivalent measurements at the Baring Head site.

[39] Taken at face value, the results show that $Cl^\bullet_{mean}$ concentrations of about 28×10^3 atoms cm^{-3} in 1994–1996 and about 9×10^3 atoms cm^{-3} in 1998–2000 are required to give the observed values of ε_A at Baring Head, provided the seasonal structure of the $Cl^\bullet$ sink remains the same. A larger value of $Cl^\bullet_{mean}$ would be possible in 1998–2000 if some unknown mechanism reduced the $Cl^\bullet$ seasonal cycle amplitude, perhaps by increasing the winter minimum of $Cl^\bullet$ concentration.

[40] The results therefore suggest that $Cl^\bullet_{mean}$ has a likely value of $18 \pm 9 \times 10^3$ atoms cm^{-3} in the MBL over open ocean (where the uncertainty arises from the observed range of ε_A). The resulting size of the global MBL $Cl^\bullet$ sink is 25 ± 12 Tg y^{-1}. This value would enrich ^{13}C in atmospheric CH_4 by 2.6 ± 1.2 ‰, and would reduce the global CH_4 turnover time by 0.4 ± 0.2 years if not compensated for by reductions in other CH_4 sink strengths or increases in source strengths. This $Cl^\bullet$ sink is significant, but has not yet been included in global CH_4 budgets.

[41] **Acknowledgments.** We thank Hilary Spencer (University of Reading) for providing the composite El Niño and La Niña SST data and Jeff Cole (University of Reading) for help with inclusion of surface methane emissions in the UM. We thank Sander Houweling (National Institute for Space Research, Netherlands) for providing the GAMeS scenario fields. This work was supported by the New Zealand Foundation for Research, Science and Technology under contract C01X0204.

References

Allan, W., M. R. Manning, K. R. Lassey, D. C. Lowe, and A. J. Gomez (2001a), Modeling the variation of $\delta^{13}C$ in atmospheric methane: Phase ellipses and the kinetic isotope effect, *Global Biogeochem. Cycles*, *15*, 467–481.

Allan, W., D. C. Lowe, and J. M. Cainey (2001b), Active chlorine in the remote marine boundary layer: Modeling anomalous measurements of $\delta^{13}C$ in methane, *Geophys. Res. Lett.*, *28*, 3239–3242.

Allan, W., D. C. Lowe, A. J. Gomez, H. Struthers, and G. W. Brailsford (2005), Interannual variation of ^{13}C in tropospheric methane: Implications for a possible atomic chlorine sink in the marine boundary layer, *J. Geophys. Res.*, *110*, D11306, doi:10.1029/2004JD005650.

Bergamaschi, P., D. C. Lowe, M. R. Manning, R. Moss, T. Bromley, and T. S. Clarkson (2001), Transects of atmospheric CO, CH_4, and their isotopic composition across the Pacific: Shipboard measurements and validation of inverse models, *J. Geophys. Res.*, *106*, 7993–8011.

Craig, H. (1957), Isotopic standards for carbon and oxygen and correction factors for mass spectrometric analysis of carbon dioxide, *Geochim. Cosmochim. Acta*, *12*, 133–149.

Cullen, M. J. P., and T. Davies (1991), Conservative split-explicit integration scheme with fourth-order horizontal advection, *Q. J. R. Meteorol. Soc.*, *117*, 993–1002.

Dlugokencky, E. J., S. Houweling, L. Bruhwiler, K. A. Masarie, P. M. Lang, J. B. Miller, and P. P. Tans (2003), Atmospheric methane levels off: Temporary pause or a new steady-state?, *Geophys. Res. Lett.*, *30*(19), 1992, doi:10.1029/2003GL018126.

Etheridge, D. M., L. P. Steele, R. J. Francey, and R. L. Langenfelds (1998), Atmospheric methane between 1000 A.D. and present: Evidence of anthropogenic emissions and climatic variability, *J. Geophys. Res.*, *103*, 15,979–15,993.

Ferretti, D. F., J. B. Miller, J. W. C. White, K. R. Lassey, D. C. Lowe, and D. M. Etheridge (2007), Stable isotopes provide revised global limits of aerobic methane emissions from plants, *Atmos. Chem. Phys.*, *7*, 237–241.

Gregory, A. R., and V. West (2002), The sensitivity of a model's stratospheric tape recorder to the choice of advection scheme, *Q. J. R. Meteorol. Soc.*, *128*, 1827–1846.

Heimann, M. (1995), The global atmospheric tracer model TM2, *Tech. Rep. 10*, Dtsch. Klimarechenzentrum, Hamburg, Germany.

Houweling, S., F. Dentener, and J. Lelieveld (1998), The impact of nonmethane hydrocarbon compounds on tropospheric chemistry, *J. Geophys. Res.*, *103*, 10,673–10,696.

Houweling, S., T. Röckmann, I. Aben, F. Keppler, M. Krol, J. F. Meirink, E. J. Dlugokencky, and C. Frankenburg (2006), Atmospheric constraints on global emissions of methane from plants, *Geophys. Res. Lett.*, *30*, L15821, doi:10.1029/2006GL026162.

Keppler, F., J. T. G. Hamilton, M. Brass, and T. Röckmann (2006), Methane emissions from terrestrial plants under aerobic conditions, *Nature*, *439*, 187–191.

Kirschbaum, M. U. F., D. Bruhn, D. M. Etheridge, J. R. Evans, G. D. Farquhar, R. M. Gifford, K. I. Paul, and A. J. Winters (2006), A comment on the quantitative significance of aerobic methane release by plants, *Functional Plant Biol.*, *33*, 521–530.

Lassey, K. R., D. M. Etheridge, D. C. Lowe, A. M. Smith, and D. F. Ferretti (2006), Centennial evolution of the atmospheric methane budget: What do the carbon isotopes tell us?, *Atmos. Chem. Phys. Disc.*, *6*, 4995–5038.

Leonard, B. P., A. P. Lock, and M. K. MacVean (1995), The NIRVANA scheme applied to one-dimensional advection, *Methods Heat Fluid Flow*, *5*, 341–377.

Morimoto, S., S. Aoki, T. Nakazawa, and T. Yamanouchi (2006), Temporal variations of the carbon isotopic ratio of atmospheric methane at Ny Ålesund, Svalbard from 1996 to 2004, *Geophys. Res. Lett.*, *33*, L01807, doi:10.1029/2005GL024648.

Platt, U., W. Allan, and D. C. Lowe (2004), Hemispheric average Cl concentrations from $^{13}C/^{12}C$ ratios in atmospheric methane, *Atmos. Chem. Phys.*, *4*, 2393–2399.

Pole, V. D., M. L. Gallani, P. R. Rowntree, and R. A. Stratton (2000), The impact of new physical parameterizations in the Hadley Centre climate model: HadAM3, *Clim. Dyn.*, *16*, 123–146.

Prather, M., et al. (2001), Atmospheric chemistry and greenhouse gases, in *Climate Change 2001: The Scientific Basis–Contribution of Working Group I to the Third Assessment Report of the Intergovernmental Panel on Climate Change*, edited by J. T. Houghton et al., pp. 241–287, Cambridge Univ. Press, New York.

Sander, S., et al. (2003), Chemical kinetics and photochemical data for use in atmospheric studies, *Tech. Rep. Evaluation 14*, Jet Propul. Lab., Pasadena, Calif.

Saueressig, G., P. Bergamaschi, J. N. Crowley, H. Fischer, and G. W. Harris (1995), Carbon kinetic isotope effect in the reaction of CH_4 with Cl atoms, *Geophys. Res. Lett.*, *22*, 1225–1228.

Saueressig, G., J. N. Crowley, P. Bergamaschi, C. Brühl, C. A. M. Brenninkmeijer, and H. Fischer (2001), Carbon 13 and D kinetic isotope effects in the reactions of CH_4 with $O(^1D)$ and OH: New laboratory measurements and their implications for the isotopic composition of stratospheric methane, *J. Geophys. Res.*, *106*, 23,127–23,138.

Spencer, H., and J. M. Slingo (2003), The simulation of peak and delayed ENSO teleconnections, *J. Clim.*, *16*, 1757–1774.

Spencer, H., J. M. Slingo, and M. K. Davey (2004), Seasonal predictability of ENSO teleconnections: The role of the remote ocean response, *Clim. Dyn.*, *22*, 511–526, doi:10.1007/s00382-004-0393-1.

Spivakovsky, C. M., et al. (2000), Three-dimensional climatological distribution of tropospheric OH: Update and evaluation, *J. Geophys. Res.*, *105*, 8931–8980.

Vogt, R., P. J. Crutzen, and R. Sander (1996), A mechanism for halogen release from sea-salt aerosol in the remote marine boundary layer, *Nature*, *383*, 327–330.

Wingenter, O. W., M. K. Kubo, N. J. Blake, T. W. Smith Jr., D. R. Blake, and F. S. Rowland (1996), Hydrocarbon and halocarbon measurements as photochemical and dynamical indicators of atmospheric hydroxyl, atomic chlorine, and vertical mixing obtained during Lagrangian flights, *J. Geophys. Res.*, *101*, 4331–4340.

Wingenter, O. W., B. C. Sive, N. J. Blake, D. R. Blake, and F. S. Rowland (2005), Atomic chlorine concentrations derived from ethane and hydroxyl measurements over the equatorial Pacific Ocean: Implication for dimethyl sulfide and bromine monoxide, *J. Geophys. Res.*, *110*, D20308, doi:10.1029/2005JD005875.

W. Allan and D. C. Lowe, National Institute of Water and Atmospheric Research, Private Bag 14901, Kilbirnie, Wellington, New Zealand. (w.allan@niwa.co.nz)

H. Struthers, National Institute of Water and Atmospheric Research, Private Bag 50061, Omakau, Central Otago, New Zealand.